Knowl Inf Syst (2015) 45:751–782
DOI 10.1007/s10115-014-0789-0

REGULAR PAPER

Evaluating link prediction methods

Yang Yang · Ryan N. Lichtenwalter · Nitesh V. Chawla

Received: 29 July 2013 / Revised: 22 May 2014 / Accepted: 20 September 2014 /
Published online: 9 October 2014

Abstract Link prediction is a popular research area with important applications in a variety of disciplines, including biology, social science, security, and medicine. The fundamental requirement of link prediction is the accurate and effective prediction of new links in networks. While there are many different methods proposed for link prediction, we argue that the practical performance potential of these methods is often unknown because of challenges in the evaluation of link prediction, which impact the reliability and reproducibility of results. We describe these challenges, provide theoretical proofs and empirical examples demonstrating how current methods lead to questionable conclusions, show how the fallacy of these conclusions is illuminated by methods we propose, and develop recommendations for consistent, standard, and applicable evaluation metrics. We also recommend the use of precision-recall threshold curves and associated areas in lieu of receiver operating characteristic curves due to complications that arise from extreme imbalance in the link prediction classification problem.

Keywords Link prediction and Evaluation · Sampling · Class imbalance · Threshold curves · Temporal effects on link prediction

Y. Yang (✉) · R. N. Lichtenwalter · N. V. Chawla
Department of Computer Science and Engineering, University of Notre Dame, 384 Fitzpatrick Hall, Notre Dame, IN 46556, USA
e-mail: yyang1@nd.edu

R. N. Lichtenwalter
e-mail: rlichten@nd.edu

N. V. Chawla
e-mail: nchawla@nd.edu

Y. Yang · R. N. Lichtenwalter · N. V. Chawla
Interdisciplinary Center for Network Science and Applications, University of Notre Dame, 384 Nieuwland Hall of Science, Notre Dame, IN 46556, USA

1 Introduction

Link prediction generally stated is the task of predicting relationships in a network [3,16,21, 28,42,50]. Typically, it is approached specifically as the task of predicting new links given some set of existing nodes and links.

Existing nodes and links may be present from a prior time period, where general link prediction is useful to anticipate future behavior [22,26,45]. Alternatively, existing nodes and links may also represent some portion of the topology in a network whose exact topology is difficult to measure. In this case, link prediction can identify or substantially narrow possibilities that are difficult or expensive to determine through direct experimentation [32, 47,49]. Thus, even in domains where link prediction seems impossibly difficult or offers a high ratio of false positives to true positives, it may be useful [7,8]. Formally, we can state the link prediction problem as below (first implicitly defined in the work of [29]):

Definition 1.1 In a network $G = (V, E)$, V is the set of nodes and E is the set of edges. The link prediction task is to predict whether there is or will be a link $e(u, v)$ between a pair of nodes u and v, where $u, v \in V$ and $e(u, v) \notin E$.

Generally the link prediction problem falls into two categories:

- Predict the links that will be added to an observed network in the future. In this scenario, the link prediction task is applicable to predicting future friendship or future collaboration, for instance, and it is also informative for exploring mechanisms underlying network evolution.
- Infer missing links from an observed network. The prediction of missing links is mostly used to identify lost or hidden links, such as inferring unobserved protein–protein interactions.

The prediction of future links considers network evolution, while the inference of missing links considers a static network [29]. In either of the two scenarios, instances in which the link forms or is shown to exist compose the positive class, and instances in which the link does not form or is shown not to exist compose the negative class. The negative class represents the vast majority of the instances, and the positive class is a small minority.

1.1 The evaluation conundrum

Link prediction entails all the complexities of evaluating ordinary binary classification for imbalanced class distributions, but it also includes several new parameters and intricacies that make it fundamentally different. Real-world networks are often very large and sparse, involving many millions or billions of nodes and roughly the same number of edges. Due to the resulting computational burden, *test set sampling* is common in link prediction evaluation [3,28,33]. Such sampling, when not properly reflective of the original distribution, can greatly increase the likelihood of biased evaluations that do not meaningfully indicate the true performance of link predictors. The selected *evaluation metric* can have a tremendous bearing on the apparent quality and ranking of predictors even with proper testing distributions [41]. The *directionality* of links also introduces issues that do not exist in typical classification tasks. Finally, for tasks involving network evolution, such as predicting the appearance of links in the future, the classification process involves *temporal aspects*. Training and testing set constructs must appropriately address these nuances.

To better describe the intricacies of evaluation in the link prediction problem, we first depict the framework for evaluation [26,38,39,52] in Fig. 1. Computations occur within

Fig. 1 Link prediction and evaluation. The *black color* indicates snapshots of the network from which link prediction features are calculated (feature network). The *gray color* indicates snapshots of the network from which the link prediction instances are labeled (label network). We can observe all links at or before time t, and we aim to predict future links that will occur at time $t + 1$

network snapshots based on particular segments of data. Comparisons among predictors require that evaluation encompasses precisely the same set of instances whether the predictor is unsupervised or supervised. We construct four network snapshots:

- Training features: data from some period in the past, G_{t-x} up to G_{t-1}, from which we derive feature vectors for training data.
- Training labels: data from G_t, the last training-observable period, from which we derive class labels, whether the link forms or not, for the training feature vectors.
- Testing features: data from some period in the past up to G_t, from which we derive feature vectors for testing data. Sometimes it may be ideal to maintain the window size that we use for the training feature vector, so we commence the snapshot at G_{t-x+1}. In other cases, we might want to be sure not to ignore effects of previously existing links, so we commence the snapshot at G_{t-x}.
- Testing labels: data from G_{t+1}, from which we derive class labels for the testing feature vector. These data are strictly excluded from inclusion in any training data.

A classifier is constructed from the training data and evaluated on the testing data. There are always strictly divided training and testing sets, because G_{t+1} is never observable in training.

Note that for supervised methods, the division of the training data into a feature and label network is not strictly necessary. Edges from the training data may be used to calculate features for instances with a positive class label, and missing edges in the training data might be used to calculate features for instances with negative class labels (Fig. 2). Nonetheless, division into a feature and label network may increase both the freshness and power of the data being modeled, because the links that appear are recent and selected according to the underlying evolution process. Testing data must *always* be divided in feature and label networks where labels are drawn from unobserved data in G_{t+1}.

Test set sampling is a common practice in link prediction evaluation [3,25,26,28,33,35,44,45,52]. Link prediction should be evaluated with a complete, unsampled test set whenever possible. Randomly removing and subsequently predicting "test edges" should be a last resort in networks where multiple snapshots do not exist. Even in networks that do not evolve, such as protein–protein interaction networks, it is possible to use high-confidence and low-confidence edges to construct different networks to more effectively evaluate models. Removing and predicting edges can remove information from the original network in unpredictable ways [46], and the removed information has the potential to affect prediction methods differently. More significantly, in longitudinal networks, randomly sampling edges for testing from a single data set in a supervised approach reflects prediction performance with respect to a random process instead of the true underlying regulatory mechanism.

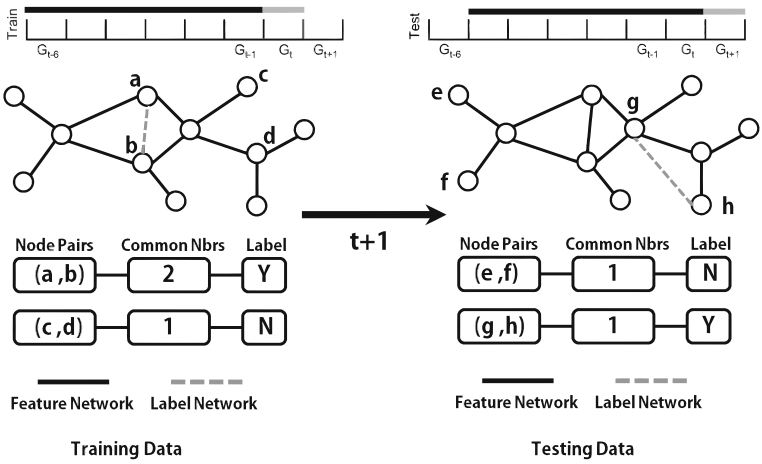

Fig. 2 Link prediction and evaluation toy example. This graph provides a toy example for the construction of training and testing sets in the link prediction problem. *Black links* correspond to the *black period* in Fig. 1, from which link prediction features were extracted. *Gray links* correspond to the *gray* future period in Fig. 1, which is used to label link prediction instances. Based on the *black* observed network, we find that the *common neighbors* values for (a, b) and (c, d) are 2 and 1, respectively. Based on the *gray* label network, we know that the link between a and b forms and the link between c and d does not form. The same methodology is applied to construct the testing data

The reason sampling seems necessary, and a primary reason link prediction is such a challenging domain within which to evaluate and interpret performance, is extreme class imbalance. We extensively analyze issues related to sampling in Sect. 4 and cover the significance of class imbalance on evaluation in Sect. 3.3. Fairly and effectively evaluating a link predictor in the face of imbalance requires determining which evaluation metric to use (Sects. 3, 6 and 7), whether to restrict the enormous set of potential predictions, and how best to restrict the set if so.

Another issue is directionality, for which there is no analog in typical classification tasks. In undirected networks, the same method may predict two different results for a link between v_a and v_b depending on the order in which vertices are presented. There must be one final judgment of whether the link will form, but that judgment differs depending on arbitrary assignment of source and target identities. We expand upon this in Sect. 3.4.

All of these issues impede the production of fair, comparable results across published methods. Perhaps even more importantly, they interfere with rendering judgments of performance that indicate what we might really expect of our prediction methods in deployment scenarios. It is difficult to compare from one paper to the next, and many frequently employed evaluation methods produce results that are unfairly favorable to a particular method or otherwise unrepresentative of expected deployment performance. We seek to provide a reference for important issues to consider and a set of recommendations to those performing link prediction research.

1.2 Contributions

We explore a range of issues and challenges that are germane to the evaluation of link predictors. Some of them are discussed in our previous work [27], of which this paper is a substantial expansion. We introduce several formalisms entirely absent from the previous

work and provide much more principled coverage of underlying issues and challenges with evaluating link prediction methods. In addition to more complete coverage of previously published topics, the extension includes the following significant advances over existing work:

- Additional data sets for stronger empirical demonstration.
- Theoretical proof of several statements surrounding evaluation.
- Discussion of the advantages and disadvantages of another popular metric of link prediction evaluation, the top K predictive rate.
- Exploration of evaluation characteristics when considering link prediction according to temporal distance. This is related to the existing study of evaluation characteristics when considering link prediction according to geodesic distance.

The point of this work is not to illustrate the superiority of one method of link prediction over another, which distinguishes it from most previous link prediction publications. Our objective is to identify fair and effective methods to evaluate link prediction performance. Overall, our contributions are summarized as follows:

- We discuss the challenges in evaluating link prediction algorithms.
- We empirically demonstrate the effects of test set sampling on link prediction evaluation and offer related proofs.
- We demonstrate that commonly used evaluation metrics lead to deceptive conclusions with respect to link prediction results. We additionally show that precision-recall curves are a fair and consistent way to view, understand, and compare link prediction results.
- We propose guidelines for a fair and effective framework for link prediction evaluation.

2 Preliminaries

2.1 Data and methods

We report all results on four publicly available longitudinal data sets. We will hence refer to these data sets as Condmat [37], DBLP [11], Enron [24], and Facebook [51]. They are constructed by moving through sequences of collaboration events (Condmat and DBLP) or communication events (Enron and Facebook). In Condmat and DBLP, each collaboration of k individuals forms an undirected k-clique with weights in inverse linear proportion to k. The detailed information about these data sets are presented in Table 1. These networks are weighted and undirected.

We use three different link prediction methods, and each method represents a different modeling approach. The preferential attachment predictor [5,6,36] uses degree product and represents predictors based on node statistics. The Adamic/Adar predictor [2] represents common neighbors predictors. The PropFlow predictor [26] represents predictors based on paths and random walks.

Table 1 Network characteristics

Networks	Condmat	DBLP	Enron	Facebook
Nodes	13,873	3,215	16,922	1,829
Edges	55,269	9,816	34,825	13,838
Density	5.74e−4	1.90e−3	2.00e−4	8.27e−3

We emphasize here that the point of this work is not to illustrate the superiority of one method of link prediction over another. It is instead to demonstrate that the described effects and arguments have real impacts on performance evaluation. If we show that the effects pertain in at least one network, it follows that they may exist in others and must be considered.

2.2 Definitions and terminology

Network: A network is represented as $G = (V, E)$, where V is the set of nodes and E is the set of edges. For two nodes $u, v \in V$, $e(u, v) \in E$ if there is a link between nodes u and v.

Neighbors: In a network $G = (V, E)$, for a node u, $\Gamma(u) = \{v|(u, v) \in E\}$ represents the set of neighbors of node u.

Link prediction: The link prediction task in a network $G = (V, E)$ is to determine whether there is or will be a link $e(u, v)$ between a pair of nodes u and v, where $u, v \in V$ and $e(u, v) \notin E$.

Common neighbors: For two nodes, u and v with sets of neighbors $\Gamma(u)$ and $\Gamma(v)$, respectively, the set of their common neighbors is defined as $\Gamma(u) \cap \Gamma(v)$, and the cardinality of the set is $|\Gamma(u) \cap \Gamma(v)|$. Often as $|\Gamma(u) \cap \Gamma(v)|$ grows, the likelihood that u and v will be connected also increases [36].

Adamic/Adar: In the link prediction problem, the Adamic/Adar [2] metric is defined as below, where $n \in \Gamma(u) \cap \Gamma(v)$ is the set of common neighbors of u and v:

$$AA(u, v) = \sum_{n \in \Gamma(u) \cap \Gamma(v)} \frac{1}{\log |\Gamma(n)|}$$

Preferential attachment: The Preferential Attachment [5] metric is the multiplication of the degrees of nodes u and v:

$$PA(u, v) = |\Gamma(u)||\Gamma(v)|$$

PropFlow: The PropFlow [26] method corresponds to the probability that a restricted, outward-moving random walk starting at u ends at v using link weights as transition probabilities. It produces a score PropFlow(u, v) that can serve as an estimation of the likelihood of new links.

Geodesic distance: The shortest path length ℓ between two given nodes u and v.

Prediction terminology: **TP** stands for *true positives*, **TN** stands for *true negatives*, **FP** stands for *false positives*, and **FN** stands for *false negatives*. **P** stands for *positive instances*, and **N** stands for *negative instances*.

Sensitivity/true positive rate:

$$\text{Sensitivity} = \frac{|TP|}{|TP| + |FN|}$$

Specificity/true negative rate:

$$\text{Specificity} = \frac{|TN|}{|FP| + |TN|}$$

Precision:

$$\text{Precision} = \frac{|TP|}{|TP| + |FP|}$$

*R*ecall:

$$\text{Recall} = \frac{|TP|}{|TP| + |FN|}$$

Fallout/false-positive rate: The false-positive rate (fallout in information retrieval) is defined as below:

$$\text{Fallout} = \frac{|FP|}{|FP| + |TN|}$$

Accuracy:

$$\text{Accuracy} = \frac{|TP| + |TN|}{|P| + |N|}$$

Top K Predictive Rate/R-precision: The top K predictive rate is the percentage of correctly classified positive samples among the top K instances in the ranking produced by a link predictor $\mathcal{P}$. We denote the top K predictive rate as TPR_K, where K is a definable threshold. TPR_K is equivalent to R-precision in information retrieval.

ROC: The receiver operating characteristic (ROC) represents the performance trade-off between true positives and false positives at different decision boundary thresholds [14,34].

AUROC: Area under the ROC curve.

Precision-recall curve: Precision-recall curves are also threshold curves. Each point corresponds to a different score threshold with a different precision and recall value [10].

AUPR: Area under the precision-recall curve.

3 Evaluation metrics and existing challenges

Evaluation metrics typically used in link prediction overlap those used in any binary classification task. They can be divided into two broad categories: fixed-threshold metrics and threshold curves. Fixed-threshold metrics suffer from the limitation that some estimate of a reasonable threshold must be available in the score space. In research contexts, where we are curious about performance without necessarily being attached to any particular domain or deployment, such estimates are generally unavailable. Threshold curves, such as the receiver operating characteristic (ROC) curve [14,34] and derived curves like cost curves [13] and precision-recall curves [10], provide alternatives in these cases.

3.1 Fixed-threshold metrics

Fixed-threshold metrics rely on different types of thresholds: prediction score, percentage of instances, or number of instances. In link prediction specifically, there are additional constraints. Some link prediction methods produce poorly calibrated scores. For instance, it often may not hold that two vertices with a degree product of 10,000 are 10 times as likely to form a new link as two with a degree product of 1,000. This is not critical when the goal of the model is to rank; however, when the scores of link predictors are poorly calibrated, it is difficult to select an appropriate threshold for any fixed-threshold performance evaluation metric. A concrete and detailed example is provided in Sect. 6, where we find that even a minor change of threshold value can lead to a completely different evaluation of link prediction models.

In Fig. 3 we provide the probability density functions and cumulative density functions for two prediction methods (Adamic/Adar and Preferential Attachment) on DBLP. For ease of interpretation, we use the inverse values of Preferential Attachment and Adamic/Adar,

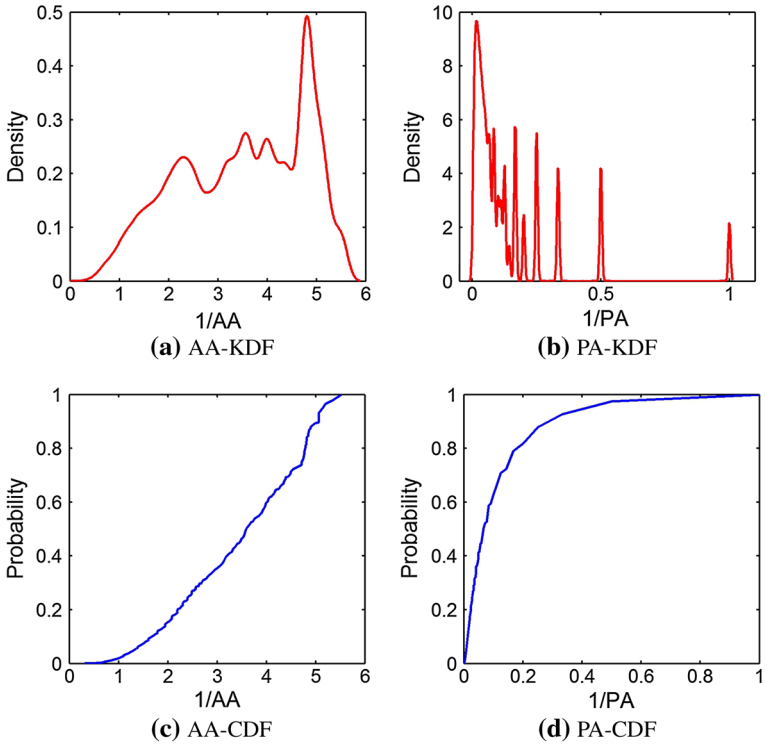

Fig. 3 Kernel density function and cumulative density function

so smaller values of Preferential Attachment and Adamic/Adar indicate higher likelihood of occurrence. In Fig. 3 we observe that preferential Attachment and Adamic/Adar have different types of distributions. This makes it difficult to identify a meaningful threshold based on normalized prediction score. Any attempt to select a value-based threshold will produce an unfair comparison between these two prediction methods.

A cardinality-based threshold is also problematic. We shall presently advocate exploring links by geodesic distance ℓ. Within this paradigm, it makes little sense to speak about the TPR_K results as a percentage of the total number of potential links in ℓ. Resources to explore potential links in model deployment scenarios are unlikely to change because the potential positives happen to span a larger distance. It is appropriate to use percentages with TPR_K only when $\ell = 2$ or $\ell \leq \infty$ and only when there is a reasonable expectation that K is logical within the domain. On the other hand, when using an absolute number of instances, if the data do not admit a trivially simple class boundary, we set classifiers up for unstable evaluation by presenting them with class ratios of millions to one and taking infinitesimal K. In Sect. 6, we discuss TPR_K evaluation in greater detail.

While *accuracy* [3,15,50], *precision* [3,21,38,50,52,53], *recall* [3,20,21,50,56], and top K equivalents [4,12,38,52,53] are used commonly in link prediction literature, we need to be cautious when results come only in terms of fixed thresholds.

3.2 Threshold curves

Due to the rarity of cases when researchers are in possession of reasonable fixed thresholds, threshold curves are commonly used in the binary classification community to express

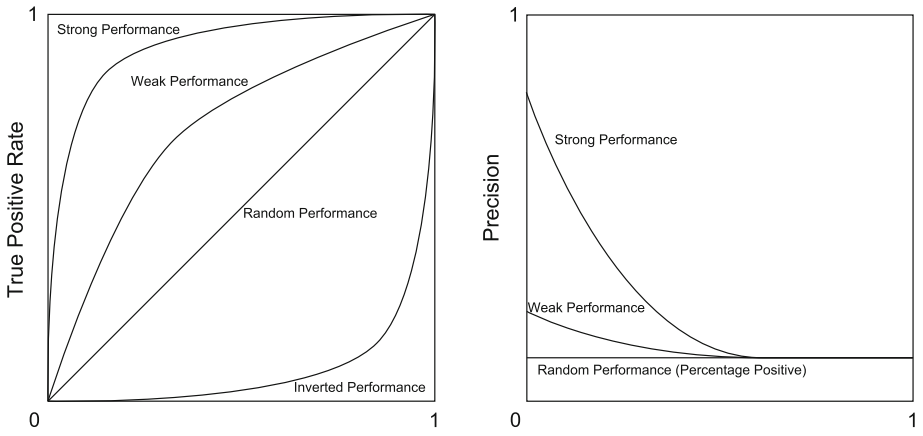

(a) ROC Curve **(b)** Precision-Recall Curve

Fig. 4 A visualization of the two threshold curves used throughout this paper

results. They are especially popular when the class distribution is highly imbalanced and hence are used increasingly commonly in link prediction evaluation [4,7,9,17,26,48,52,55]. Threshold curves admit their own scalar measures, which serve as a single summary statistic of performance. The ROC curve shows the true positive rate with respect to the false-positive rate at all classification thresholds, and its area (AUROC) is equivalent to the probability of a randomly selected positive instance appearing above a randomly selected negative instance in score space. The precision-recall (PR) curve shows precision with respect to recall at all classification thresholds. It is connected to ROC curves such that one precision-recall curve dominates another if and only if the corresponding ROC curves show the same domination [10]. We will use ROC curves and precision-recall curves to illustrate our points and eventually argue for the use of precision-recall curves and areas. Figure 4 illustrates a depiction of the two curve metrics.

3.3 Class imbalance

In typical binary classification tasks, classes are approximately balanced. As a result, we can calculate expectations for baseline classifier performance. For instance, the expected accuracy $\left(\frac{TP+TN}{TP+FP+TN+FN}\right)$, precision $\left(\frac{TP}{TP+FP}\right)$, recall $\left(\frac{TP}{TP+FN}\right)$, AUROC, and AUPR of a random classifier, an all-positive classifier, and an all-negative classifier are 0.5.

Binary classification problems that exhibit class imbalance do not share this property, and the link prediction domain is an extreme example. The expectation for each of the classification metrics diverges for random and trivial classifiers. Accuracy is problematic because its value approaches unity for trivial predictors that always return false. Correct classification of rare positive instances is simultaneously more important since those instances represent exceptional cases of high relative interest. Classification is an exercise in optimizing some measure of performance, so we must not select a measure of performance that leads to a useless result. ROC curves offer a baseline random performance of 0.5 and penalize trivial predictors when appropriate. Optimizing ROC optimizes the production of class boundaries that maximize *TP* while minimizing *FP*. Precision and precision-recall curves offer baseline

performance calibrated to the class balance ratio, and this can present a soberer view of performance.

3.4 Directionality

In undirected networks, an additional methodological parameter pertains in the task of evaluation, which is rarely reported in the literature. In directed networks, an *ordered* pair of vertices uniquely specifies a prediction, because order implies edge direction. In undirected networks, the lack of directionality renders the order ambiguous since two pairs map to one edge. For any given edge, there are two potentially different prediction outputs. For some prediction methods, such as those based on node properties or common neighbors, the prediction output remains the same irrespective of ordering, but this is not true in general. Most notably, many prediction methods based on paths and walks, such as PropFlow [26] and Hitting Time [28], implicitly depend on notions of source and target.

Definition 3.1 In an undirected network $G = (V, E)$, for a link prediction method $\mathcal{P}$, if there exists a pair of nodes u and v such that $\mathcal{P}(u, v) \neq \mathcal{P}(v, u)$, then $\mathcal{P}$ is said to be *directional*.

Contemplate Fig. 5 with the goal of predicting a link between v_a and v_b. Consider the percentage of $\ell = 2$ paths starting from v_a that reach v_b versus the percentage of $\ell = 2$ paths starting from v_b that reach v_a. Clearly, all $\ell = 2$ paths originating at v_b reach v_a, whereas only a third of the $\ell = 2$ paths originating at v_a reach v_b. In a related vein, consider the probability of reaching one vertex from another in random walks. Clearly, all walks starting at v_b that travel at least two hops must reach v_a, whereas the probability of reaching v_b from v_a in two hops is lower. Topological prediction outputs may diverge whenever v_a and v_b are in different automorphism orbits within a shared connected component.

This raises the question of how to determine the final output of a method that produces two different outputs depending on the input. Any functional mapping from two values to a single-value suffices. Selection of an optimal method depends on both the predictor and the scenario and is outside the scope of this paper. Nonetheless, it is important for reasons of reproducibility not to neglect this question when describing results for directional predictors.

The approach consistent with the process for directed networks would be to generate a ranked list of scores that includes predictions with each node alternately serving as source and destination. This approach is workable in a deployment scenario, since top-ranked outputs may be selected as predicted links regardless of the underlying source and target. It is not feasible as a research method for presenting results, however, because the meaning of the resulting threshold curves is ambiguous. There is also no theoretical reason to suspect any sort of averaging effect in the construction of threshold curves.

To emphasize this empirically, we computed AUROC in the undirected Condmat data set for two methods using the PropFlow predictor (predicting links within 2-hop distance). The PropFlow predictor is directional, so for two nodes u and v, it is possible that

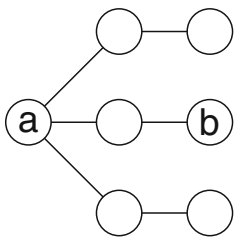

Fig. 5 A simple undirected graph example to illustrate that predictions for a link from v_a to v_b may differ according to which vertex is considered as the source

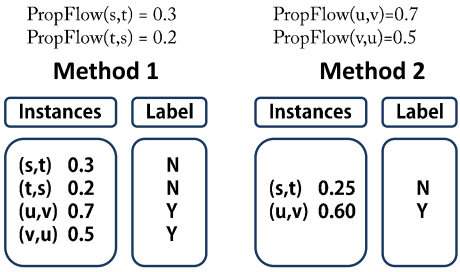

Fig. 6 Directionality toy example. In this example, for node pairs (s, t) and (u, v), PropFlow$(s, t) \neq$ PropFlow(t, s) and PropFlow$(u, v) \neq$ PropFlow(v, u). In one evaluation method, the curve is generated from the ranked list of predictions over both vertex orderings. In the other method, the arithmetic mean of the prediction on the two underlying orderings is used to generate the curve. In the Condmat data set, these two methods have different AUROCs: 0.610 and 0.625, respectively

PropFlow $(u, v) \neq$ PropFlow (v, u). The first method includes a prediction in the output for both underlying orderings, and the resulting area is 0.610. The second method computes the arithmetic mean of the predictions from the two underlying orderings to produce a single final prediction for the rankings, and the resulting area is 0.625 (Fig. 6).

4 Test set sampling and class imbalance

Test set sampling is popular in link prediction domains, because sparse networks usually include only a tiny fraction of the $O(|V|^2)$ links supported by V. Each application of link prediction must provide outputs for what is essentially the entire set of $\binom{|V|}{2}$ links. For even moderately sized networks, this is an enormously large number that places unreasonable practical demands on processing and even storage resources. As a result, there are many sampling methods for link prediction testing sets. One common method is selecting a subset of edges at random from the original complete set [3,45,48,52,53,56]. Another is to select only the edges that span a particular geodesic distance [26,31,43,44,55]. Yet another is to select edges so that the subdistribution composed by a particular geodesic distance is approximately balanced [35,52]. Finally, any number of potential methods can select edges that present a sufficient amount of information along a particular dimension [28,33], for instance selecting only the edges where each member vertex has a degree of at least 2.

When working with threshold-based measures, any sampling method that removes negative class instances above the decision threshold can unpredictably raise most information retrieval measures. Precision is inflated by the removal of false positives. In top K measures, recall is inflated by the opportunity for additional positives to appear above the threshold after the negatives are removed. This naturally affects the harmonic mean, F-measure. Accuracy is affected by any test set modification since the number of incorrect classifications may change. Clearly, we cannot report meaningful results with these threshold-based measures when performing any type of sampling on the test set. The question is whether it is fair to sample the test set when evaluating with threshold curves.

At first it may seem that subsampling negatives from the test set has no negative effects on ROC curves and areas. There is a solid theoretical basis for this belief, but issues specific to link prediction relating to extreme imbalance cause problems in practice. We will first describe these problems, and why using evaluation methods involving extreme subsampling

are problematic. Then, we will show that test set sampling actually creates what we believe is a much more significant problem with the testing distribution.

4.1 Impact of sampling on ROC

Theoretically, ROC curves and their associated areas are unaffected by changes in class distribution alone. This is a source of great appeal, since it renders consistent judgments even as imbalance becomes increasingly extreme. Consequently, it is theoretically possible to fairly sample negatives from the test set without affecting ROC results. The proper way to model fair random removals of test instances closest to the actual ROC curve construction step is as random selection without replacement from the unsorted or sorted list of output scores. As long as the distribution remains stable in the face of random removals, the ROC curve and area will remain unchanged.

In practice, we do not want to waste the effort necessary to generate lists of output scores only to actually examine a fractional percentage of them. We must instead find a way to transfer our fair model of random removals in the ranked list of output scores to a network sampling method while theoretically preserving all feature distributions. The solution is to randomly sample potential edges. Given a network in which our original evaluation strategy was to consider a test set with every potential edge based on the previously observed network, we generate an appropriately sized random list of edges that do not exist in the test period.

As suggested by Hoeffding's inequality [19], in machine learning the test set has finite-sample variance. When the test set is sampled, the performance is as likely to be pleasantly surprising as unpleasantly surprising, though likely not to be surprising at all [1]. We provide a concrete mathematical proof specifically in the link prediction domain. Theoretically, we can prove that with a random sampling ratio p of negative instances to final testing set size, the variance of measured performance increases as p decreases.

Theorem 4.1 *For any link predictor $\mathcal{P}$, the variance of measured performance increases when the negative class sample percentage p decreases.*

Proof For a specific predictor $\mathcal{P}$, we assume that among all N negative instances there are C instances that can be classified correctly by $\mathcal{P}$ while the other $N - C$ instances cannot be classified correctly by $\mathcal{P}$.

Based on the fact that we randomly sample Np negative instances for inclusion in the final test set, the number of negative instances that can be detected by predictor $\mathcal{P}$ among these Np negative instances is a random variable X that has probability mass function:

$$P(X = x) = \frac{\binom{C}{x}\binom{N-C}{Np-x}}{\binom{N}{Np}}$$

Trivially, X follows a *Hypergeometric* distribution and the variance of X is:

$$\mathrm{Var}(X) = \frac{C(N-C)p(1-p)}{(N-1)}$$

Since the performance X/Np has variance following:

$$\mathrm{Var}\left(\frac{X}{Np}\right) = \frac{C(N-C)(1-p)}{N^2(N-1)p} \tag{1}$$

it follows that when p decreases $\mathrm{Var}\left(\frac{X}{Np}\right)$ increases.

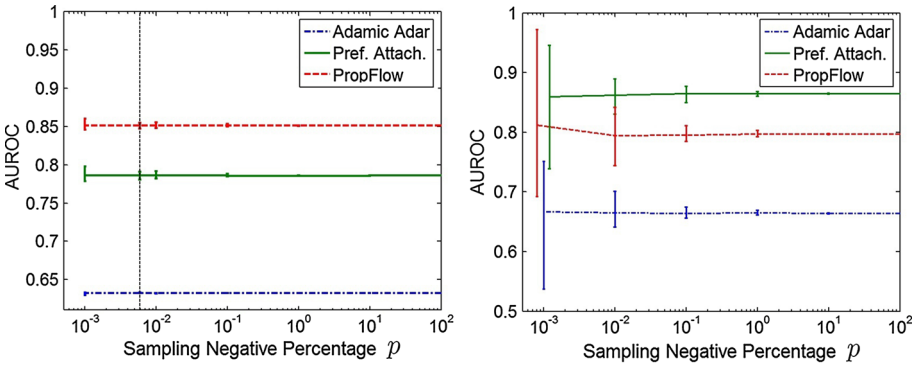

(a) Condmat **(b)** Facebook

Fig. 7 Effect of sampling of negative class instances in the testing set for unsupervised classifiers. In (**a**), the *vertical line indicates* class balance. We separate the *error bars* for different methods at the point $p = 10^{-3}$ for comparison purposes. With decreasing p, the variance of AUROC for a link predictor increases. When the negative class percentage is between 10^{-1} and 10^{2}, the mean value of AUROC for a link predictor does not change much, because the number of negative instances is still much larger than the number of positive instances. In the Condmat network, the imbalance ratio is around 10^{5}, so even when the negative class sample percentage is 10^{-1} the imbalance ratio in the sampled test set is around 10^{2}. When the negative class sample percentage is low enough (i.e., 10^{-2}), the mean value of AUROC is unstable (see results of DBLP and Enron in Fig. 8)

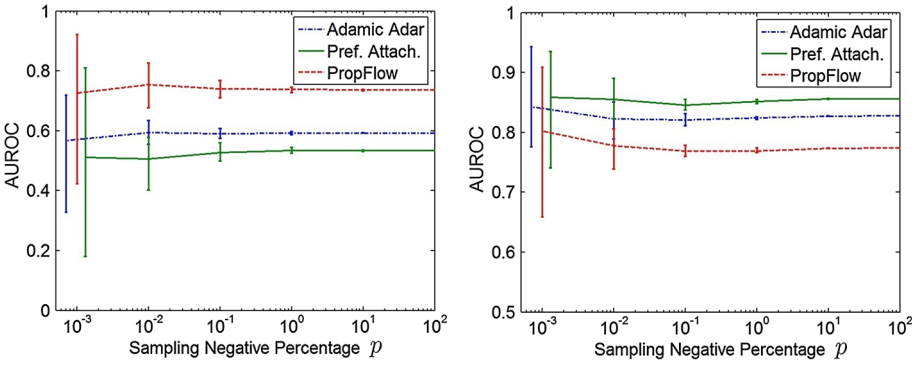

(a) DBLP **(b)** Enron

Fig. 8 Effect of sampling negative class instances in test sets on AUROC in supervised learning. We separate the *error bars* for different methods at the point $p = 10^{-3}$ for comparison purposes

From Eq. 1, we can observe that the variance of the measured performance increases linearly with $\frac{1}{p}$.

We demonstrate the results of this random sampling strategy empirically in Fig. 7 (unsupervised learning) and Fig. 8 (supervised learning). We conduct these experiments for AUROC but not for AUPR, because precision-recall curves respond to the modifications of the testing set if the class distribution changes [10]. The experimental settings follow. We explore the effect of sampling of negative class instances in the testing set. We include in our experiments six sampling rates: 10^{-3}, 10^{-2}, 10^{-1}, 10^{0}, 10^{1}, and 10^{2} %. For each sampling rate, we randomly sample the testing set 100 times and calculate the AUROC for each. Thus for each

sampling rate, we have 100 AUROC scores. In Figs. 7 and 8, we report the mean, minimum, and maximum of these scores.

The AUROC remains stable down to 1 % of the negative class in Condmat and only down to 10 % of the negative class in Facebook for unsupervised learning. Below this, it destabilizes. While stability to 1 % sampling in Condmat may seem quite good, it is critical to note that the imbalance ratios of link prediction in large networks are such that 1 % of the complete original test set often still contains an unmanageably large number of instances. Similarly in Fig. 8, the AUROC remains stable only down to 10 % negative class sampling for both DBLP and Enron in supervised learning circumstance.

The dashed vertical line shows the AUROC for sampling that produces a balanced test set. The area deviates by more than 0.007 for PropFlow and more than 0.01 for preferential attachment, which may exceed significant variations in performance across link predictors. Further sampling causes even greater deviations. These deviations are not a weakness of the AUROC itself but are indicative of instability in score rankings within the samples. This instability does not manifest itself uniformly, and it may be greater for some predictors than for others. In Condmat in Fig. 7, preferential attachment exhibits greater susceptibility to the effect, while in Facebook in Fig. 7, PropFlow has the greatest susceptibility. The ultimate significance of the effect depends upon many factors, such as sampling percentage of negative class, properties of the predictor, and network size. From the proof of Theorem 4.1, we can observe that the variance is also influenced by the negative instances number N. This is validated empirically by variations in stability across negative class sample ratios in different data sets. Condmat is stable down to 1 % sampling of negative class instances while DBLP, Enron, and Facebook are stable only down to 10 % sampling of negative class instances. In sparse networks $G = (V, E)$, we can prove that the variance changes according to the order of magnitude of $|V|^2$.

Definition 4.1 Let a network $G = (V, E)$ be described as sparse if it maintains the property $|E| = k|V|$ for some constant $k \ll |V|$.

Corollary 4.2 *Given constant sampling ratio p, and that at most $|V|$ nodes may join the sparse network, and that the prediction ability of $\mathcal{P}$ does not change in different sparse networks, G_α and G_β:*

$$\frac{Var_\alpha}{Var_\beta} \in \Theta\left(\frac{|V_\beta|^2}{|V_\alpha|^2}\right)$$

where Var_α is the performance variance of the link predictor $\mathcal{P}$ in the sparse network G_α, Var_β is the performance variance of the link predictor $\mathcal{P}$ in the sparse network G_β, and $|V_\alpha|$ and $|V_\beta|$ are node counts in the network G_α and G_β.

Proof As we have proved in Theorem 4.1, the variance of the performance of $\mathcal{P}$ can be written as:

$$\mathrm{Var}\left(\frac{X}{Np}\right) = \frac{C(N-C)(1-p)}{N^2(N-1)p}$$

Thus, the variances Var_α and Var_β can be written as:

$$\mathrm{Var}_\alpha = \frac{C_\alpha(N_\alpha - C_\alpha)(1-p_\alpha)}{N_\alpha^2(N_\alpha-1)p_\alpha}$$

$$\mathrm{Var}_\beta = \frac{C_\beta(N_\beta - C_\beta)(1-p_\beta)}{N_\beta^2(N_\beta-1)p_\beta}$$

Due to the assumption that the prediction ability of $\mathcal{P}$ does not change in G_α and G_β, we can write $\frac{\text{Var}_\alpha}{\text{Var}_\beta}$ as:

$$\frac{\text{Var}_\alpha}{\text{Var}_\beta} = \frac{\frac{C_\alpha(N_\alpha - C_\alpha)(1-p_\alpha)}{N_\alpha^2(N_\alpha-1)p_\alpha}}{\frac{C_\beta(N_\beta - C_\beta)(1-p_\beta)}{N_\beta^2(N_\beta-1)p_\beta}} = \frac{\frac{(1-p_\alpha)}{(N_\alpha-1)p_\alpha}}{\frac{(1-p_\beta)}{(N_\beta-1)p_\beta}}$$

Additionally, we know that $p_\alpha = p_\beta$, so we can rewrite $\frac{\text{Var}_\alpha}{\text{Var}_\beta}$ as:

$$\frac{\text{Var}_\alpha}{\text{Var}_\beta} = \frac{\frac{(1-p_\alpha)}{(N_\alpha-1)p_\alpha}}{\frac{(1-p_\beta)}{(N_\beta-1)p_\beta}} = \frac{N_\beta - 1}{N_\alpha - 1}$$

Now we prove that $N_\alpha \in \Theta(|V_\alpha|^2)$, $N_\beta \in \Theta(|V_\beta|^2)$: The number of all possible links in network G is $\frac{|V|^2-|V|}{2}$, so for a sparse network the missing links, $|E|^C$, is $\frac{|V|^2-|V|}{2} - k|V| \in \Theta(|V|^2)$. Let $V^{'}$ nodes and $E^{'}$ edges join the network in the future. Since the evolved network $G^{'}$ is still a sparse network and $V^{'} \leq |V|$, we know that $|V| + |V^{'}| \leq 2|V| \in \Theta(|V|)$ and $|E| + |E^{'}| \in \Theta(|V|)$. The negatives are given as $|(E \bigcup E^{'})^C| \in \Theta(|V|^2)$. Trivially, we have

$$N_\alpha - 1 \in \Theta(|V_\alpha|^2)$$
$$N_\beta - 1 \in \Theta(|V_\beta|^2)$$

And we know that $\frac{\text{Var}_\alpha}{\text{Var}_\beta} \in \Theta(\frac{|V_\beta|^2}{|V_\alpha|^2})$ □

We prove that theoretically the variance changes approximately with the order of magnitude of $|V|^2$, and this is illustrated in both Figs. 7 and 8. Figure 8 shows that our conclusions regarding the impact of negative class sampling with unsupervised predictors also hold for supervised predictors. In Fig. 7, the Condmat data set has a larger number of nodes than the Facebook data set, and unsurprisingly, we observe that for the same predictor with the same negative class sample ratio, the variance in Facebook is much larger than in Condmat. For supervised learning, the size of DBLP is smaller than Enron and the variance for Enron is much smaller than for DBLP.

This theoretical demonstration and the empirical results show grave danger in relying on results of sampled test sets in the link prediction domain. One of the most common strategies is to undersample negatives in the test set so that it is balanced. In link prediction, class balance ratios, often easily exceeding thousands to one, are likely to leave resampled test sets that do not admit sufficiently stable evaluation for meaningful results.

4.2 The real testing distribution

We must understand what performance we report when we undersample link prediction test sets. Undersampling is presumably part of an attempt at combating unmanageable test set sizes and describing the performance of the predictor on the network as a whole. This type of report is common, and issues of stability aside, it is theoretically valid. We question, however, whether the results that it produces actually convey useful information. Figure 10 compares AUROC overall to the AUROC achievable in the distinct subproblem created by dividing the task by geodesic distance.

We first consider the results for the preferential attachment predictor. The general conclusion across all data sets is that the apparent achievable performance is dramatically higher in

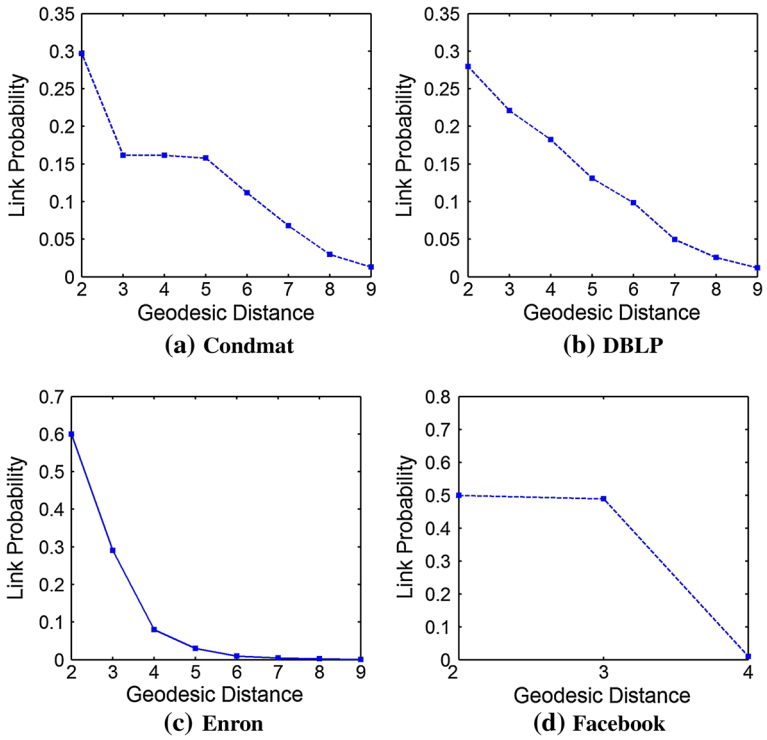

Fig. 9 Probability of edges E_ℓ created between nodes ℓ geodesic hops away

the complete sets of potential edges than the performance in the sets restricted by distance. The extreme importance of geodesic distance in determining link formation correlates highly with any successful prediction method. The high-distance regions contain very few positives and effectively append a set of trivially recognizable negatives to the end. This increases the probability of a randomly selected positive appearing above a randomly selected negative, the AUROC. This phenomenon is described as the locality of link formation in growing networks [23,30,40,54]. In Fig. 9, we study the distribution of geodesic hops induced by each new links for four data sets. The number of new links decays exponentially with increasing hop distance between nodes.

Beyond the statistics presented in Fig. 10, we compare the AUROCs of two surrogate scenarios. In the first scenario, we simulate the $\ell = 2$ subproblem, denoted as P_{sub}. In the second scenario, we simulate the complete link prediction problem $\ell \leq \infty$, denoted as P_{full}. There are p_s positive instances and n_s negative instances in P_{sub}, and there are p_f positive instances and n_f negative instances in P_{full}. We designate a parameter α to control the performance of the predictor $\mathcal{P}$. In the simulation, the positive instances are randomly allocated among the top α slots in the ranking list. Additionally to simplify the simulation, we assume that the prediction method $\mathcal{P}$ has the same performance in these two problems. Because P_{sub} is a subproblem of P_{full}, in order to simulate P_{full} more precisely, we require further details as follows:

– Among p_f positive instances, p_s of them are randomly allocated within the top $\alpha(p_s + n_s)\beta$ slots in the ranking list, where the parameter β is introduced to simulate the impact of non-trivially recognizable negatives on the ranking of p_s positives in subproblem P_s.

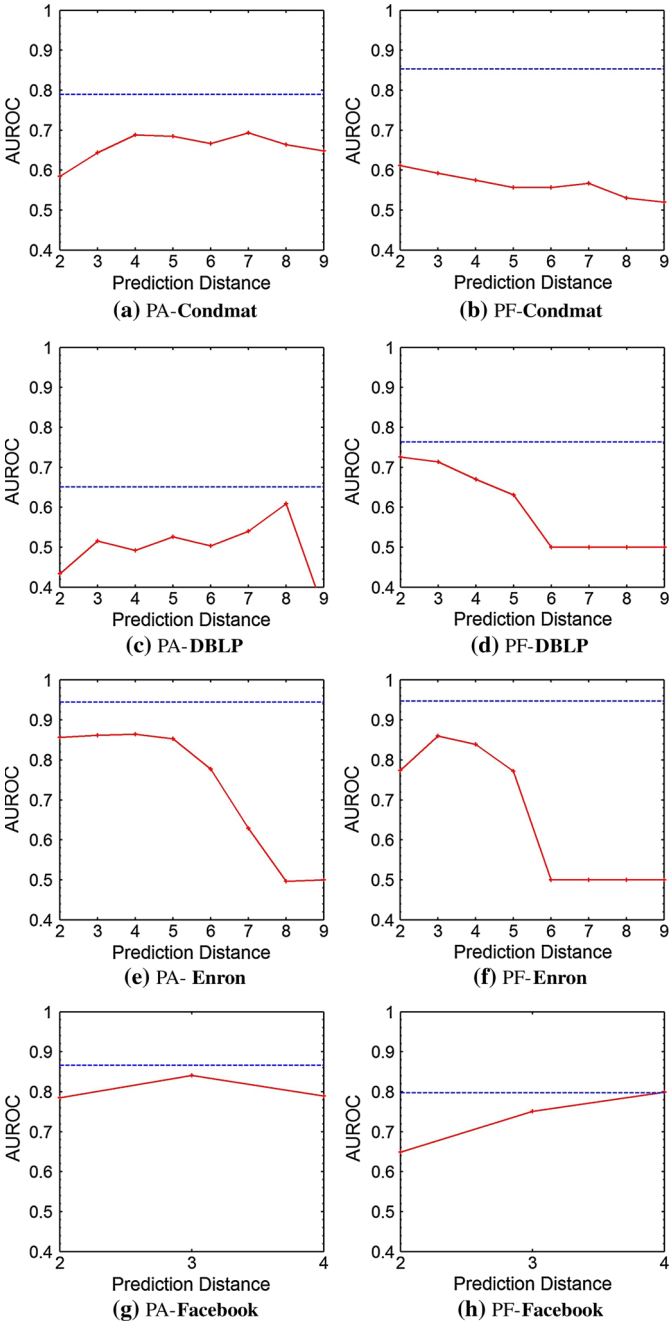

Fig. 10 ROC curve performance of the preferential attachment and PropFlow link predictors over each neighborhood. The results of Adamic/Adar are not included because the Adamic/Adar method only has descriptive power for node pairs within two hops. The *horizontal line* represents the performance apparent by considering all potential links. We compare AUROC overall to the AUROC achievable in the distinct subproblem created by dividing the task by geodesic distance ℓ. The *red line* represents the AUROC for each subproblem (color figure online)

Table 2 Surrogate comparisons

α	β				
	10	20	30	40	50
0.2	8 sigmas	6 sigmas	5 sigmas	3 sigmas	2 sigmas
0.3	8 sigmas	6 sigmas	5 sigmas	3 sigmas	2 sigmas
0.4	9 sigmas	7 sigmas	5 sigmas	4 sigmas	2 sigmas
0.5	9 sigmas	7 sigmas	5 sigmas	4 sigmas	2 sigmas
0.6	9 sigmas	7 sigmas	6 sigmas	4 sigmas	2 sigmas
0.7	9 sigmas	7 sigmas	6 sigmas	4 sigmas	2 sigmas
0.8	9 sigmas	7 sigmas	6 sigmas	4 sigmas	2 sigmas
0.9	9 sigmas	7 sigmas	6 sigmas	4 sigmas	3 sigmas

The α parameter controls the performance of link predictors, and lower values of α indicate higher performance of link predictors. The β parameter simulates the impact of non-trivially recognizable negatives on the ranking of p_s positives in subproblem P_s. In the simulation, we demonstrate that based on the AUROC the performance on the full link prediction problem ($\ell \leq \infty$) is significantly better (H_0 rejected at 2 sigmas) than the subproblem ($\ell \leq 2$). This observation made in surrogate scenarios is validated by the real-world experiments in Fig. 10

– Then, $p_f - p_s$ positive instances are randomly allocated within the top $\alpha(p_f + n_f)$ slots in the ranking list.

The parameter α is designed to simulate the performance of the predictor, while the parameter β is designed to simulate the impact of appending negatives. Table 2 shows the results of this comparison. In order to comprehensively measure the statistical significance of differences between P_f and P_s, we compare the AUROCs of P_f to those of P_s by 100,000 simulations under different settings of α and β. The numbers of p_s, n_s, p_f, and n_f are taken from the DBLP data set.

In Table 2, the predictability α values correspond to a high AUROC, 0.9, and to a worst-case AUROC, 0.5. When the impact of appending negatives is small (i.e., $\beta = 10$), the AUROC of P_f is most dramatically greater than the AUROC of P_s, with p value less than 0.0001. Even if the impact of appending negatives is large (i.e., $\beta = 50$), the AUROC of P_f is much larger than that of P_s, with p-value at most 0.048. The above observation is not significantly influenced by the performance of the predictor $\mathcal{P}$.

In Fig. 10, we can observe that different prediction methods have different behaviors for varying ℓ subproblems. In the DBLP data set, preferential attachment is unstable across geodesic distances while PropFlow exhibits monotonic behavior. This is because the preferential attachment method is inherently "non-local" in its judgment of link formation likelihood. Additionally, as discussed earlier, the difference between AUROC in $\ell \leq \infty$ and AUROC in distinct subproblems (i.e., $\ell = 2$) is diminished when the size of the network decreases.

The effect is exaggerated for PropFlow and for other ranking methods that inherently scale according to distance, such as rooted PageRank and Katz. In such cases, the ROC curve for the amalgamated data approximates concatenation of the individual ordered outputs, which inherently places the distances with higher imbalance ratios at the end where they inflate the overall area. Figure 10 shows the effect for the PropFlow prediction method on the right.

For PropFlow, the apparent achievable performance in Condmat is 36.2% higher for the overall score ordering than for the highest of the individual orderings! This result also has important implications from a practical perspective. In the Condmat network, PropFlow appears to have a higher AUROC than preferential attachment ($\ell \leq \infty$), but the *only* distance

at which it outperforms preferential attachment is the 2-hop distance. Preferential attachment is a superior choice for the other distances in cases where the other distances matter. These details are hidden from view by ROC space. They also illustrate that the performance indicated by overall ROC is not meaningful with respect to deployment expectations and that it conflates performance across neighborhoods with a bias toward rankings that inherently reflect distance.

Consider the data distribution of the link prediction problem used in this paper. In Condmat, there are 148.2 million negatives and 29,898 positives. The ratio of negatives to positives is 4,955 to 1. There are 1,196 positives and 214,616 negatives in $\ell = 2$. To achieve a 1 to 1 ratio with random edge sampling, statistical expectation is for 43.3 2-hop negatives to remain. The 2-hop neighborhood contains 30 % of all positives, so clearly it presents the highest baseline precision. That border is the most important to capture well in classification, because improvements in $\ell = 2$ discrimination are worth much more than improvements at higher distances. 16 % of all positives are in the $\ell = 3$ subproblem, so the same argument applies with it versus higher distances.

The real data distribution on which we report performance when we perform this sampling is the relatively easy boundary described by the highly disparate $\ell = 2$ positives and high-distance negatives. Figure 11 further substantiates this point by illustrating the minimal effect of selectively filtering all negatives from low-distance neighborhoods. We know that performance in the $\ell = 2$ is most significant because of the favorable class ratio and that improvements in defining this critical boundary offer the greatest rewards. Simultaneously, as the figure shows, in Condmat we can entirely remove all $\ell = 2$ test negatives with only a 0.2 % effect on the AUROC for two predictors from entirely different families. We must remove all $\ell \leq 4$ test negatives before the alteration becomes conspicuous, yet these are the significant boundary instances.

Since we also know that data distributions do not affect ROC curves, we can extend this observation even when no sampling is involved: Considering the entire set of potential links in ROC space evaluates prediction performance of low-distance positives versus high-distance negatives. We must instead describe performance within the distribution of $\ell = 2$ positives and negatives and select predictors that optimize this boundary.

4.3 Case study on Kaggle sampling

Of the described sampling methods, only uniform random selection from the complete set of potential edges preserves the testing distribution. Though questionable for meaningful evaluation of deployment potential, it is at least an attempt at unbiased evaluation. One recently employed alternative takes another approach to sampling, aggressively undersampling negatives from over-represented distances and preserving a much higher proportion of low-distance instances. The Kaggle link prediction competition [35] undersampled the testing set by manipulating the amount of sampling from each neighborhood to maintain approximate balance within the neighborhoods. The distribution of distances exhibited by the 8,960 test edges is shown in Fig. 12.

Consider the results of Fig. 12 against the results of fair random sampling in the Condmat network. Unless Kaggle has an incredibly small effective diameter, it is impossible to obtain this type of distribution. It requires a sampling approach that includes low-distance edges from the testing network with artificially high probability. While this selective sampling approach might seem to better highlight some notion of average boundary performance across neighborhoods, it is instead meaningless because it creates a testing distribution that would never exist in deployment. The Kaggle competition disclosed that the test set was balanced.

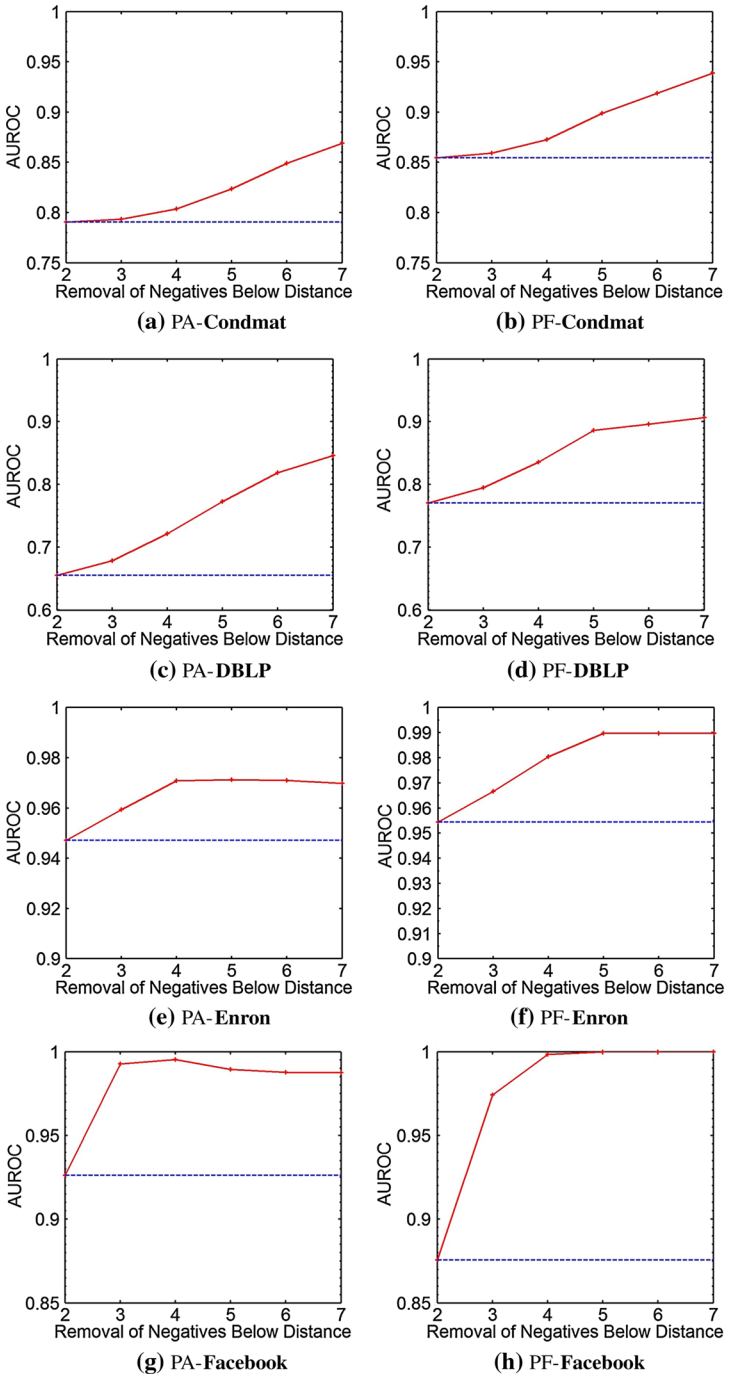

Fig. 11 Effect of removing negative instances from increasingly distant potential links. The *horizontal line* represents the base AUROC on the unsampled test set. This figure illustrates the minimal effect of selectively filtering all negatives from low-distance neighborhoods. As we observe with the increase of ℓ, the AUROC increases when all negative instances below ℓ are removed

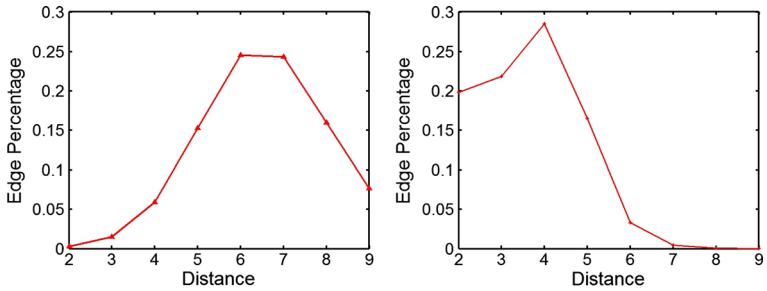

(a) Condmat **(b)** Kaggle

Fig. 12 Distribution of distances in test sets

In a deployment scenario, it is impossible to provide to a prediction method a balance of positives and negatives from each distance, because that would require knowledge of the target of the prediction task itself.

More significantly, the Kaggle approach is unfair and incomparable because the original distribution is not preserved, and there is no reason to argue for one arbitrary manipulation of distance prevalence over another. Simultaneously, the AUROC will vary greatly according to each distributional shift. It is even possible to predictably manipulate the test set to achieve an arbitrary AUROC through such a sampling approach. Any results obtained via such a testing paradigm are inextricably tied to the sampling decisions themselves, and the sampling requires the very results we are predicting in a deployment scenario. As a result, Kaggle AUROCs may not be indicative of real achievable performance or even of a proper ranking of models in a realistic prediction task.

To empirically explore the differences between a fair random sampling strategy and the Kaggle sampling strategy, we provide the distributions of distances in different data sets using both sampling strategies. Additionally, we also compare the AUROC achievable in two sampling strategies. In Fig. 13, we compare the differences of distance distributions when using fair random sampling and Kaggle sampling, while in Table 3 we provide ROC performances (AUROC) of prediction methods under these two sampling strategies.

In Table 3, we can see that the apparent achievable performance using the Kaggle sampling strategy is remarkably higher, up to 25 %, than the performance achievable by fair random sampling. The performance discrepancy between fair random sampling and Kaggle sampling depends upon several factors, such as the prediction method, network size, and the geodesic distribution of positive instances. Here, we will explore the observations made in Table 3.

- *Geodesic distribution*. Increasing ℓ increases the difficulty of the prediction subproblem due to increasing imbalance. The Kaggle sampling maintains approximate balance within each neighborhood, greatly reducing the difficulty of the link prediction task. This is the cause for apparent performance improvements when using the Kaggle sampling strategy.
- *Preferential attachment*. Preferential attachment ignores the impact of geodesic distance between nodes, so it fails to penalize distant potential links appropriately. Kaggle sampling removes many high-distance negative instances, and most positive instances within high-distance neighborhoods have high preferential attachment scores. As a result, preferential attachment benefits particularly from Kaggle sampling.
- *PropFlow*. PropFlow considers the influence of geodesic distance on the formation of links. In Condmat or DBLP, when there are more positive instances spanning high distances, the Kaggle strategy unfairly penalizes path-based measures such as PropFlow.

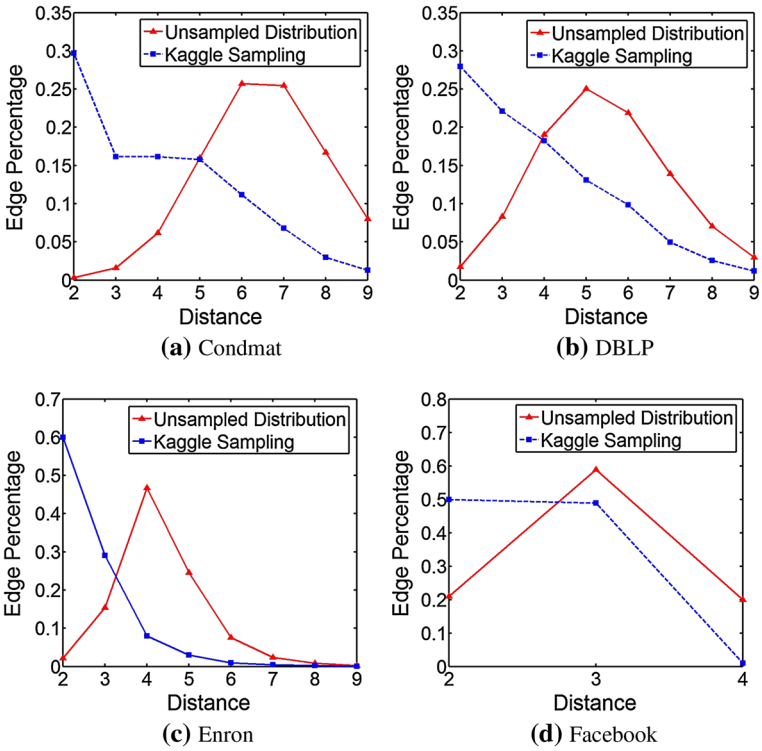

Fig. 13 Comparison between fair random sampling and Kaggle sampling

Table 3 ROC area (AUROC)

Predictor	Condmat		DBLP		Enron		Facebook	
	Fair	Kaggle	Fair	Kaggle	Fair	Kaggle	Fair	Kaggle
Pref. Attach.	0.79	**0.88**	0.65	**0.86**	0.94	**0.97**	0.86	**0.98**
PropFlow	0.85	**0.86**	0.76	**0.89**	0.95	**0.99**	0.80	**0.99**
Adamic Adar	0.63	**0.63**	0.62	**0.63**	0.79	**0.80**	0.66	**0.75**

Bold values help distinguish the results of Kaggle and fair methodology

Contrarily when positive instances reside in low-distance neighborhoods, such as Enron and Facebook, PropFlow fares better.

– *Adamic Adar*. The Adamic/Adar method only has descriptive power within the $\ell = 2$ subproblem. In data sets where high-distance links are sampled more often, the apparent performance of Adamic/Adar is strikingly and unfairly impacted.

5 New nodes

There are two fundamentally different ways to generate test sets in link prediction. The first is to create a set of potential links by examining the predictor network and selecting all pairs for which no edge exists. Positives are those among the set that subsequently appear in the testing network, and negatives are all others. The second is to use the testing network to

generate the set of potential links. Positives are those that exist in the testing network but not in the training network, and negatives are those that could exist in the testing network but do not. The subtle difference lies in whether or not the prediction method is faced with or penalized for links that involve *nodes* that do not appear during training time.

The choice we should make depends on how the problem is posed. If we are faced with the problem of returning a most confident set of predictions, then new nodes in the testing network are irrelevant. Although we could predict that an existing node will connect to an unobserved node, we cannot possibly predict what node the unobserved node will be.

If we are faced with the problem of answering queries, then the ability to handle new nodes is an important aspect of performance. On the one hand, we could offer a constant response, either positive or negative, to all queries regarding unfamiliar nodes. The response to offer and its effect on performance depend on the typical factors of cost and expected class distribution. On the other hand, some prediction methods may support natural extensions to provide a lesser amount of information in such cases. For instance, preferential attachment could be adapted to assume a degree of 1 for unknown nodes. Path-based predictors would have no basis to cope with this scenario whatsoever. In supervised classification, any such features become missing values and the algorithm must support such values.

Evaluating with potential links drawn from the testing network is problematic for decomposing the problem by distance since the distance must be computed from single-source shortest paths based on the pretend removal of the link that appears only in the testing network. Since distance is such a crucial player in determining link likelihood in most networks, this would nonetheless be an early step in making a determination about link formation likelihood in any case, so its computation for creating divided test sets is probably unavoidable. Given the extra complexity introduced by using potential link extraction within the testing network, we opt for determining link pairs for testing based on training data unless there is a compelling reason why this is unsatisfactory. This decision only has the potential to exclude links that are already known to be impossible to anticipate from training data, so it necessarily has the same effect across any set of predictors.

6 Top K predictive rate

Though we caution trusting results that come only in terms of fixed thresholds metrics, some of these fixed thresholds metrics have significant real-world applications. A robust threshold curve metric exhibits the trade-off between sensitivity and specificity. A desirable property of a good fixed-threshold metric is that higher score implies an increase both in *sensitivity* and *specificity*. In this section, we discuss the *top K predictive rate* [29], which we shall write as TPR_K, and explore its evaluation behavior in the link prediction problem. Top K equivalent evaluation metrics have been discussed previously in the work of [21,38,52], and this measure is well known as R-precision from information retrieval. We provide a proof of one property of TPR_K that is important in link prediction. Based on this proof, we explore the restrictions of TPR_K in evaluating the link prediction performance.

We denote the set of *true positives* as **TP**, the set of *true negatives* as **TN**, the set of *false positives* as **FP**, the set of *false negatives* as **FN**, the set of all positive instances as **P**, and the set of all negative instances as **N**.

Definition 6.1 TPR_K is the percentage of correctly classified positive samples among the top K instances in the ranking by a specified link predictor $\mathcal{P}$.

This metric has the following property:

Theorem 6.1 *When $K = |\mathbf{P}|$ in the link prediction problem, sensitivity and specificity are linearly dependent on TPR_K.*

Proof By definition, we know:

$$TPR_K = \frac{|\mathbf{TP}|}{K}, \text{sensitivity} = \frac{|\mathbf{TP}|}{|\mathbf{P}|}$$

So the equivalence $K = |\mathbf{P}|$ allows us to trivially conclude that TPR_K and sensitivity are identical. We can write *specificity* as:

$$\text{specificity} = \frac{|\mathbf{TN}|}{|\mathbf{N}|}$$

When $K = |\mathbf{P}|$, by definition $|\mathbf{FP}| = K - |\mathbf{TP}|$, because we predict that all top K are positive instances, and we can conclude that:

$$\begin{aligned}
&|\mathbf{P}| - |\mathbf{TP}| = |\mathbf{FP}| \\
&\rightarrow (1 - TPR_K)|\mathbf{P}| = |\mathbf{FP}| \\
&\rightarrow |\mathbf{TN}| + (1 - TPR_K)|\mathbf{P}| = |\mathbf{TN}| + |\mathbf{FP}| \\
&\rightarrow \frac{|\mathbf{TN}|}{|\mathbf{N}|} + (1 - TPR_K)|\mathbf{P}|\frac{1}{|\mathbf{N}|} = 1 \\
&\rightarrow \text{specificity} = 1 - (1 - TPR_K)\frac{|\mathbf{P}|}{|\mathbf{N}|}
\end{aligned}$$

From this, we see that *specificity* increases monotonically with the increase in TPR_K and is linearly dependent on TPR_K.

In Fig. 14, we provide the TPR_K performance of predictors on Condmat, DBLP, Enron, and Facebook. The vertical line indicates the performance of a naive algorithm that draws samples as edges uniformly at random from all instances. Although the top K predictive rate can provide a good performance estimation of link prediction methods when K is appropriately selected, we still cannot recommend it as a primary measurement. If $|\mathbf{P}|$ is known, then K may be set to that, but in real applications it is often impossible to know or even approximate the number of positive instances in advance, so K is not specifiable. From Fig. 14, we can see that different values of K lead to different evaluations and even rankings of link prediction methods. Figure 14c shows that a small difference in K will lead to a ranking reversal of the preferential attachment and PropFlow predictors. TPR_K is a good metric for the link prediction task when the value of K is appropriately selected, but evaluation results are too sensitive to use arbitrary K.

7 The case for precision-recall curves

ROC curves (and AUROC) are appropriate for typical data imbalance scenarios because they optimize toward a useful result and because the appearance of the curve provides a reasonable visual indicator of expected performance. One may achieve an AUROC of 0.99 in scenarios where data set sizes are relatively small (10^3 to 10^6) and imbalance ratios are relatively modest (2 to 20). Corresponding precisions are near 1. For complete link prediction in sparse networks, when every potential new edge is classified, the imbalance ratio is *lower* bounded by the number of vertices in the network [26]. ROC curves and areas can be deceptive in this

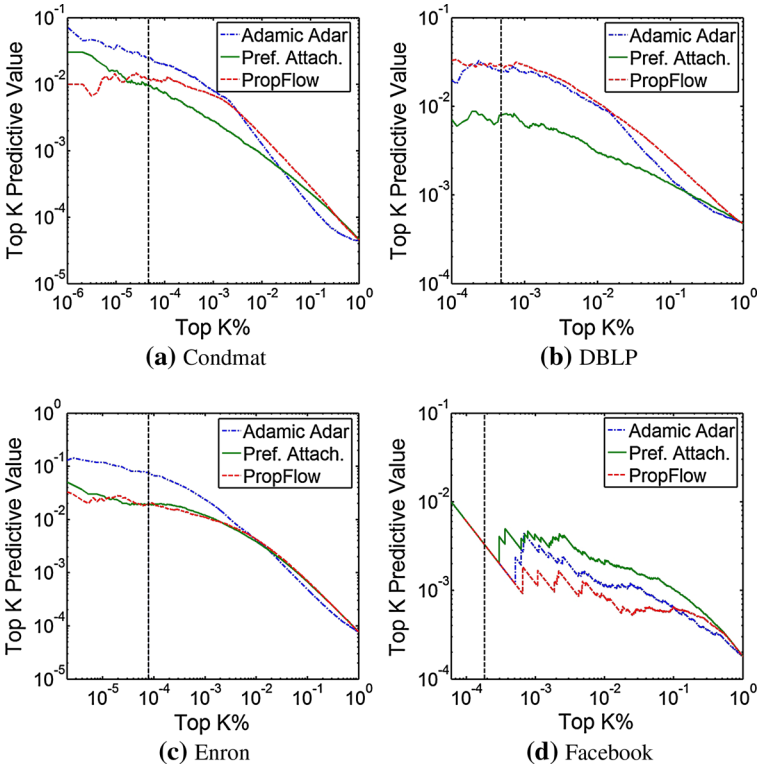

Fig. 14 Top K predictive rate. In each figure, the *vertical line* indicates that $K\% = \frac{|\mathbf{P}|}{|\mathbf{P}|+|\mathbf{N}|}$

situation. In a network with millions of vertices, even with an exceptional AUROC of 0.99, one could suffer small fractions as a maximal precision. Performance put in these terms is often considered unacceptable to researchers. In most domains, examining several million false positives to find each true positive *is* the classification problem. Even putting aside more concrete theoretical criticisms of ROC curves and areas [18] in link prediction tasks, they fail to honestly convey the difficulty of the problem and reasonable performance expectations for deployment. We argue for the use of precision-recall curves and AUPR in link prediction contexts.

7.1 Geodesic effect on link prediction evaluation

Precision-recall (PR) curves provide a more discriminative view of classification performance in extremely imbalanced contexts such as link prediction [10]. Like ROC curves, PR curves are threshold curves. Each point corresponds to a different score threshold with a different precision and recall value. In PR curves, the x axis is recall and the y axis is precision. We will now revisit a problematic scenario that arose with AUROCs and demonstrate that AUPRs present a less deceptive view of predictor performance data. Notably, and compatible with our recommendations against sampling, PR curve construction procedures will require that negatives are not subsampled from the test set. This is not computationally problematic in the consideration of distance-restricted predictions.

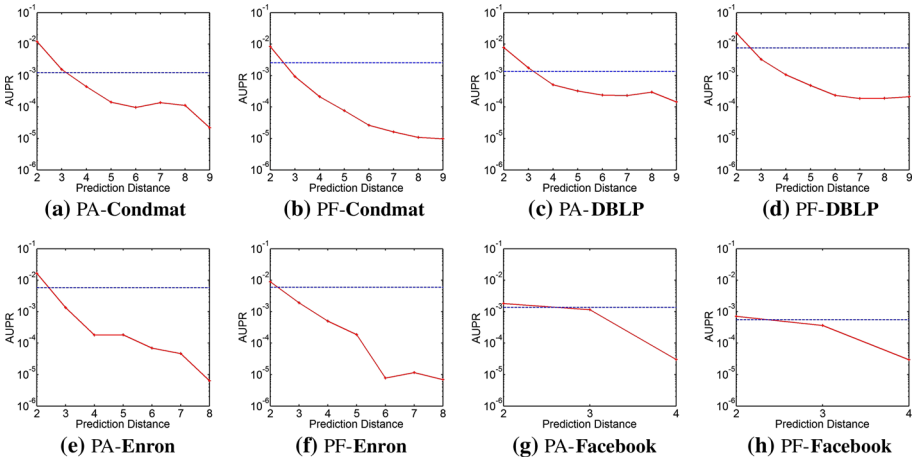

Fig. 15 Precision-recall curve performance of the preferential attachment link predictor and PropFlow link predictor over each neighborhood. The *horizontal line* represents the performance apparent by considering all potential links as a corpus

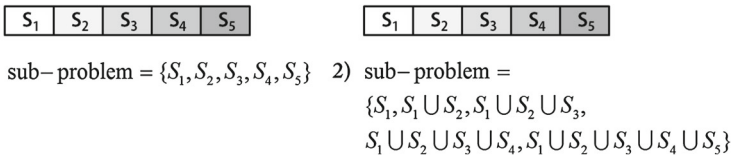

Fig. 16 Experimental configurations

Figure 15 shows that the AUPR is higher for $\ell = 2$ than it is for $\ell \leq \infty$. This also validates our proposition that increasing ℓ increases the difficulty of the prediction subproblem due to increasing imbalance, which is made in Sect. 4.3. In the underlying curves, this is exhibited as much higher precisions throughout but especially for low to moderate values of recall. Performance by distance exhibits expected monotonic decline due to increasing baseline difficulty excluding the instabilities in very high distances. Compare this to Fig. 10 where the AUROC for all potential links was much greater than for any neighborhood individually, and the apparent performance was greatest in the 7-hop distance data set. We can also observe in Fig. 15 that the PR area increases almost monotonically with increasing ℓ, which differs from the AUROC in Fig. 10.

7.2 Temporal effect on link prediction evaluation

Time has remote yet non-negligible effects on the link prediction task. In this section, we conduct two kinds of experiments. First, with a fixed training set, we compare AUROC and AUPR overall to AUROC and AUPR achievable in distinct subproblems created by dividing the task by temporal distance when the test set is sliced into 5 subsets of the same duration. Second, with a fixed training set, we compare AUROC and AUPR overall across agglomerated subproblems.

First, we divide the testing set into 5 subsets of equal temporal duration. For instance, in DBLP there are 5 years of data in the testing set, so each year of data provides one subproblem. Figure 16-1 gives an example of the experimental setting. As described in Fig. 16-1, we denote

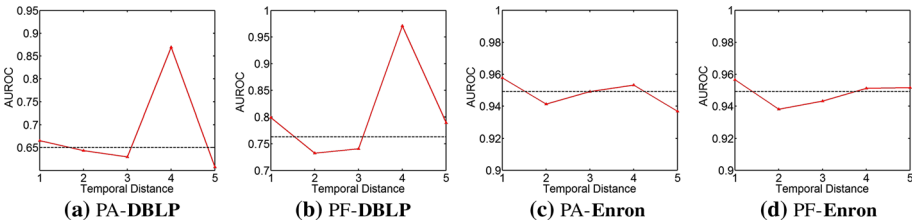

(a) PA-**DBLP** **(b)** PF-**DBLP** **(c)** PA-**Enron** **(d)** PF-**Enron**

Fig. 17 AUROC performance of preferential attachment and PropFlow over each temporal neighborhood. The *horizontal line* represents the performance apparent by considering all future potential links

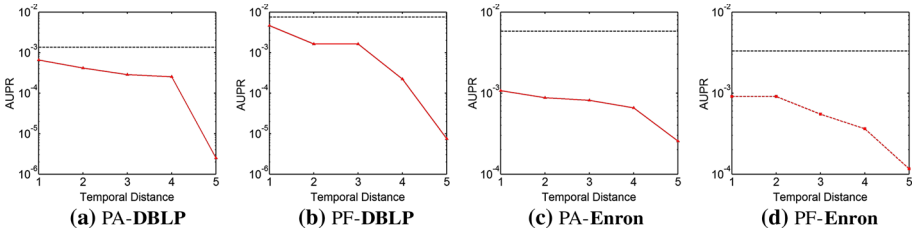

(a) PA-**DBLP** **(b)** PF-**DBLP** **(c)** PA-**Enron** **(d)** PF-**Enron**

Fig. 18 AUPR performance of preferential attachment and PropFlow over each temporal neighborhood. The *horizontal line* represents the performance apparent by considering all future potential links

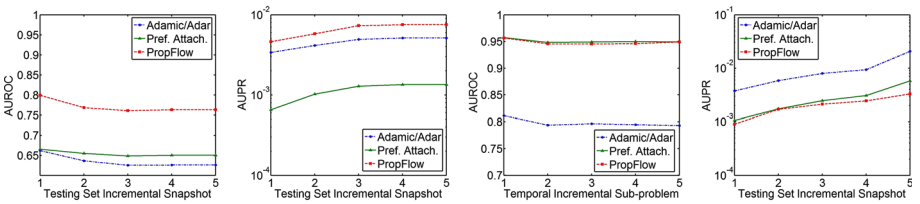

(a) ROC-**DBLP** **(b)** PR Curve-**DBLP** **(c)** ROC-**Enron** **(d)** PR Curve-**Enron**

Fig. 19 Performance of incremental temporal neighborhood. The test set temporal distance is incremental. The subproblem becomes easier when more years of data are included, because the total number of prediction candidates is fixed while the number of positive instances is increasing. The performance of a predictor should increase when the subproblem includes more data

these subproblems as S_1, S_2, S_3, S_4, and S_5. S_i increases in difficulty as i increases, because the time series is not persistent [55], and the preponderance of a node to form new links decays exponentially [23]. Based on this hypothesis, the performance of a link predictor $\mathcal{P}$ on subproblem S_i should decrease with increasing i.

In Figs. 17 and 18, we provide ROC curves and PR curves. We revisit the deceptive nature of AUROCs and demonstrate that AUPRs present a less deceptive view of performance. Based on time series analysis, the performance of a predictor should decline in the presence of high temporal distance, but AUROCs fluctuate with increasing temporal distance. The AUPRs exhibit expected monotonic decline due to increasing baseline difficulty. This finding coincides with our results in Sects. 4 and 7.1, where AUROC values fluctuate with geodesic distance and AUPR values decrease monotonically.

To emphasize these conclusions, we agglomerate the subproblems over time as shown in Fig. 16-2. The subproblem becomes easier when more years of data are included, because the total number of prediction candidates is fixed while the number of positive instances is increasing. In this way, the performance of a predictor should increase when the subprob-

lem includes more data. Figure 19 shows distinct behaviors of AUROCs and AUPRs. The AUROC values decline or are unstable while the AUPR values for all three predictors increase monotonically.

8 Conclusion

To select the best predictor, we must know how to evaluate predictors. Beyond this, we must be sure that readers do not come away from papers with the question of how new methods *actually* perform. It is more difficult to specify and explain link prediction evaluation strategies than with standard classification wherein it is sufficient to fully specify a data set, one of a few evaluation methods, and a given performance metric. In link prediction, there are many potential parameters often with many undesirable values. There is no question that the issues raised herein *can* lead to questionable or misleading results. The theoretical and empirical demonstrations should convince the reader that they *do* lead to questionable or misleading results.

Much of this paper relies upon the premise that the class balance ratio differs, even differs wildly, across distances. There are certainly rare networks where such an expectation is tenuous, but the premise holds in every network with which the authors have worked including networks from the following families: biology, commerce, communication, collaboration, and citation.

Based on our observations and analysis, we propose the following guidelines:

1. Use precision-recall curves and AUPR as an evaluation measure. In our experiments, we observe that ROC curves and AUROC can be deceptive, but precision-recall curves yield better precision in evaluating the performance of link prediction (Sects. 4.1 and 7.2).
2. Avoid fixed thresholds unless they are supplied by the problem domain. We identify limitations and drawbacks of fixed thresholds metrics, such as top K predictive rate (Sect. 6).
3. Render prediction performance evaluation by geodesic distance. In Sects. 4.2, 7, and 7.2, we observe that the performance of subproblems created by dividing the link prediction task by geodesic distance is significantly different from overall link prediction performance. In cases where temporal distance is a significant component of prediction, consider also rendering performance by temporal distance.
4. Do not undersample negatives from test sets, which will be of more manageable size due to consideration by distance. Experiments and proofs both demonstrate that undersampling negatives from test sets can lead to inaccurately measured performance and incorrect ranking of link predictors (Sect. 4).
5. If negative undersampling *is* undertaken for some reason, it must be based on a purely random sample of edges missing from the test network. It must not modify dimensions in the original distribution. Naturally, *any* sampling must be *clearly* reported. Inappropriate methods of sampling will lead to incorrect measures of link prediction performance, a fact demonstrated by Kaggle sampling as analyzed in Sect. 4.3.
6. In undirected networks, state if a method is invariant to designations of source and target. If it is not, state how the final output is produced. As we discover in Sect. 3.4, different strategies overcoming the directionality issue lead to different judgments about performance.

7. Always take care to use the same testing set instances regardless of the nature of the prediction algorithm.
8. In temporal data, the final test set on which evaluation is performed should receive labels from a subsequent, unobserved snapshot of the data stream generating the network (Sect. 7.2).
9. Consider whether the link prediction task set forth is to solve the recommendation problem or the query problem and construct test sets accordingly (Sect. 5).

Acknowledgments Research was sponsored in part by the Army Research Laboratory (ARL) and was accomplished under Cooperative Agreement Number W911NF-09-2-0053, and in part from grant #FA9550-12-1-0405 from the U.S. Air Force Office of Scientific Research (AFOSR) and the Defense Advanced Research Projects Agency (DARPA). The views and conclusions contained in this document are those of the authors and should not be interpreted as representing the official policies, either expressed or implied, of the ARL, AFOSR, DARPA or the U.S. Government. The U.S. Government is authorized to reproduce and distribute reprints for Government purposes notwithstanding any copyright notation hereon.

References

1. Abu-Mostafa YS, Magdon-Ismail M, Lin HT (2012) Learning from data: a short course. AMLBook
2. Adamic L (2001) Friends and neighbors on the web. Soc Netw 25(3):211–230
3. Al-Hasan M, Chaoji V, Salem S, Zaki M (2006) Link prediction using supervised learning. In: Proceedings of SDM'06 workshop on link analysis, counterterrorism and security
4. Backstrom L, Leskovec J (2011) Supervised random walks: predicting and recommending links in social networks. In: Proceedings of the fourth ACM international conference on Web search and data mining, pp 635–644
5. Barabási AL, Albert R (1999) Emergence of scaling in random networks. Science 286:509–512
6. Barabási A-L, Jeong H, Néda Z, Ravasz E, Schubert A, Vicsek T (2002) Evolution of the social network of scientific collaboration. Phys A Stat Mech Appl 311(3–4):590–614
7. Clauset A, Moore C, Newman MEJ (2008) Hierarchical structure and the prediction of missing links in networks. Nature 453(7191):98–101
8. Clauset A, Shalizi CR, Newman MEJ (2009) Power-law distributions in empirical data. SIAM Rev 51(4):661–703
9. Davis D, Lichtenwalter R, Chawla NV (2011) Multi-relational link prediction in heterogeneous information networks. In: Proceedings of the 2011 international conference on advances in social networks analysis and mining, pp 281–288
10. Davis J, Goadrich M (2006) The relationship between precision-recall and ROC curves. In: Proceedings of the 23rd international conference on machine learning, pp 233–240
11. Deng H, Han J, Zhao B, Yu Y, Lin CX (2011) Probabilistic topic models with biased propagation on heterogeneous information networks. In: Proceedings of the 17th ACM SIGKDD international conference on knowledge discovery and data mining, pp 1271–1279
12. Dong Y, Tang J, Wu S, Tian J, Chawla NV, Rao J, Cao H (2012) Link prediction and recommendation across heterogeneous social networks. In: Proceedings of the 2012 international conference on data mining, pp 181–190
13. Drummond C, Holte RC (2006) Cost curves: an improved method for visualizing classifier performance. Mach Learn 65(1):95–130
14. Fawcett T (2004) ROC graphs: notes and practical considerations for researchers. ReCALL 31(HPL-2003-4), pp 1–38
15. Fletcher RJ, Acevedo MA, Reichert BE, Pias KE, Kitchens WM (2011) Social network models predict movement and connectivity in ecological landscapes. Proc Natl Acad Sci 108(48):19282–19287
16. Getoor L (2003) Link mining: a new data mining challenge. ACM SIGKDD Explor Newsl 5(1):84–89
17. Goldberg DS, Roth FP (2003) Assessing experimentally derived interactions in a small world. Proc Natl Acad Sci 100(8):4372–4376
18. Hand DJ (2009) Measuring classifier performance: a coherent alternative to the area under the ROC curve. Mach Learn 77(1):103–123
19. Hoeffding W (1963) Probability inequalities for sums of bounded random variables. J Am Stat Assoc 58(301):13–30

20. Hopcroft J, Lou T, Tang J (2011) Who will follow you back? Reciprocal relationship prediction. In: Proceedings of the 20th ACM international conference on Information and knowledge management, pp 1137–1146
21. Huang Z, Li X, Chen H (2005) Link prediction approach to collaborative filtering. In: Proceedings of the 5th ACM/IEEE-CS joint in proceedings on digital libraries, pp 7–11
22. Leroy V, Cambazoglu BB, Bonchi F (2010) Cold start link prediction. In: Proceedings of the 16th ACM SIGKDD international conference on knowledge discovery and data mining, pp 393–402
23. Leskovec J, Backstrom L, Kumar R, Tomkins A (2008) Microscopic evolution of social networks. In: Proceedings of the 14th ACM SIGKDD international conference on knowledge discovery and data mining, pp 462–470
24. Leskovec J, Lang K, Dasgupta A, Mahoney M (2009) Community structure in large networks: natural cluster sizes and the absence of large well-defined clusters. Internet Math 6(1):29–123
25. Leskovec J, Huttenlocher D, Kleinberg J (2010) Predicting positive and negative links in online social networks. In: Proceedings of the 19th international conference on world wide web, pp 641–650
26. Lichtenwalter RN, Lussier JT, Chawla NV (2010) New perspectives and methods in link prediction. In: Proceedings of the 16th ACM SIGKDD international conference on knowledge discovery and data mining, pp 243–252
27. Lichtenwalter RN, Chawla NV (2012) Link prediction: fair and effective evaluation. In: IEEE/ACM international conference on social networks analysis and mining, pp 376–383
28. Liben-Nowell D, Kleinberg J (2003) The link prediction problem for social networks. In: Proceedings of the twelfth international conference on information and knowledge management, pp 556–559
29. Liben-Nowell D, Kleinberg J (2007) The link-prediction problem for social networks. J Am Soc Inf Sci Technol 58(7):1019–1031
30. Liu X, He Q, Tian Y, Lee WC, McPherson J, Han J (2012) Event-based social networks: linking the online and offline social worlds. In: Proceedings of the 18th ACM SIGKDD international conference on knowledge discovery and data mining, pp 1032–1040
31. Lu L, Zhou T (2011) Link prediction in complex networks: a survey. Phys A 390(6):1150–1170
32. Martinez ND, Hawkins BA, Dawah HA, Feifarek BP (1999) Effects of sampling effort on characterization of food-web structure. Ecology 80:1044–1055
33. Murata T, Moriyasu S (2007) Link prediction of social networks based on weighted proximity measures. In: Proceedings of the IEEE/WIC/ACM international conference on web intelligence, pp 85–88
34. Mason SJ, Graham NE (2002) Areas beneath the relative operating characteristics (roc) and relative operating levels (rol) curves: statistical significance and interpretation. Q J R Meteorol Soc 2002:2145–2166
35. Narayanan A, Shi E, Rubinstein BIP (2011) Link prediction by de-anonymization: how we won the Kaggle social network challenge. Arxiv preprint arXiv:1102.4374
36. Newman MEJ (2001) Clustering and preferential attachment in growing networks. Phys Rev Lett E 64(2):025102
37. Newman MEJ (2001) The structure of scientific collaboration networks. Proc Natl Acad Sci 98:404–409
38. O'Madadhain J, Hutchins J, Smyth P (2005) Prediction and ranking algorithms for event-based network data. ACM SIGKDD Explor Newsl 7(2):23–30
39. O'Madadhain J, Smyth P, Adamic L (2005) Learning predictive models for link formation. In: International sunbelt social network conference
40. Papadopoulos F, Kitsak M, Serrano M, Boguna M, Krioukov D (2012) Popularity versus similarity in growing networks. Nature 489(7417):537–540
41. Raeder T, Hoens TR, Chawla NV (2010) Consequences of variability in classifier performance estimates. In: Proceedings of the 10th IEEE international conference on data mining, pp 421–430
42. Sarukkai RR (2000) Link prediction and path analysis using Markov Chains. In: Proceedings of the 9th international WWW inproceedings on computer networks: the international journal of computer and telecommunications networking, pp 377–386
43. Scellato S, Mascolo C, Musolesi M, Latora V (2010) Distance matters: geo-social metrics for online social networks. In: Proceedings of the 3rd conference on online social networks, pp 8–8
44. Scellato S, Noulas A, Mascolo C (2011) Exploring place features in link prediction on location-based social networks. In: Proceedings of the 17th ACM SIGKDD international conference on knowledge discovery and data mining, pp 1046–1054
45. Scripps J, Tan PN, Chen F, Esfahanian AH (2008) A matrix alignment approach for link prediction. In: Proceedings of the 19th international conference on pattern recognition, pp 1–4
46. Stumpf MPH, Wiuf C, May RM (2005) Subnets of scale-free networks are not scale-free: sampling properties of networks. Proc Natl Acad Sci 102(12):4221–4224

47. Sprinzak E, Sattath S, Margalit H (2003) How reliable are experimental protein–protein interaction data? J Mol Biol 327(5):919–923
48. Sun Y, Han J, Aggarwal CC, Chawla NV (2012) When will it happen? Relationship prediction in heterogeneous information networks. In: Proceedings of the fifth ACM international conference on web search and data mining, pp 663–672
49. Szilágyi A, Grimm V, Arakaki AK, Skolnick J (2005) Prediction of physical protein–protein interactions. Phys Biol 2(2):S1–16
50. Taskar B, Wong MF, Abbeel P, Koller D (2003) Link prediction in relational data. In: Proceedings of the conference on neural information processing systems
51. Viswanath B, Mislove A, Cha M, Gummadi KP (2009) On the evolution of user interaction in facebook. In: Proceeding of the 2nd ACM SIGCOMM workshop on social networks, pp 37–42
52. Wang C, Satuluri V, Parthasarathy S (2007) Local probabilistic models for link prediction. In: Proceedings of the IEEE international conference on data mining, pp 322–331
53. Wang D, Pedreschi D, Song C, Giannotti F, Barabasi AL (2011) Human mobility, social ties, and link prediction. In: Proceedings of the 17th ACM SIGKDD international conference on knowledge discovery and data mining, pp 1100–1108
54. Wittie MP, Pejovic V, Deek L, Almeroth KC, Zhao BY (2010) Exploiting locality of interest in online social networks. In: Co-NEXT '10 proceedings of the 6th international conference
55. Yang Y, Chawla NV, Sun Y, Han J (2012) Predicting links in multi-relational and heterogeneous networks. In: Proceedings of the 12th IEEE international conference on data mining, pp 755–764
56. Yin Z, Gupta M, Weninger T, Han J (2010) A unified framework for link recommendation using random walks. In: Proceedings of the 2010 international conference on advances in social networks analysis and mining, pp 152–159

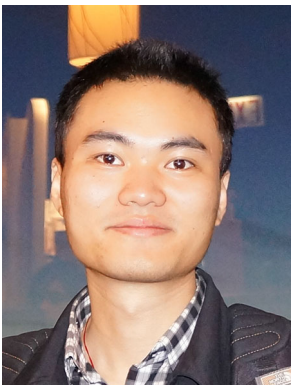

Yang Yang is currently a PhD candidate in the Department of Computer Science at the University of Notre Dame. He is a member of the iCeNSA research group and the Data, Inference, Analysis, and Learning (DIAL) research group. His principal research interest is in large-scale information and social networks. More generally, he studies data mining, statistics, and network science, with a focus on the link prediction problem, social influence analysis, and social network evolution. His research has been focused on new methodologies of predicting links in social networks and exploring underlying principles of social network evolution. He is also interested in applying network methodologies to analyze the development of complex socioeconomic systems, such as the evolution of trader alliance networks in unstable economies.

Ryan N. Lichtenwalter received his PhD in computer science in 2012 from the University of Notre Dame. He specializes in applying data mining and network science to large data sets with a particular emphasis on the link prediction problem. His dissertation was titled "Network analysis and link prediction: effective and meaningful modeling and evaluation." He has worked to maximize the transparency and reproducibility of his own work through the encapsulation of research methods in publicly available open-source software.

Nitesh V. Chawla PhD is the Frank Freimann Collegiate Chair of Engineering and the Associate Professor of Computer Science and Engineering at the University of Notre Dame. He is also the director of the Notre Dame Interdisciplinary Center on Network Science and Applications (iCeNSA), an institute focused on network and data science. His research work has led to many interdisciplinary contributions in social networks, healthcare analytics, environmental sciences, learning analytics, and media. He is an award-winning researcher and teacher, receiving prestigious recognition such as the IBM Big Analytics Award, IBM Watson Faculty Award, IEEE CIS Outstanding Early Career Award, National Academy of Engineers New Faculty Fellowship, and Outstanding Teacher Awards.